arXiv:0810.5545v1 [cond-mat.mes-hall] 30 Oct 2008

Nanogranular Thermoelectrics

Andreas Glatz[1] and I. S. Beloborodov[2]
[1]*Materials Science Division, Argonne National Laboratory, Argonne, Illinois 60439, USA*
[2]*Department of Physics and Astronomy, California State University Northridge, Northridge, CA 91330, USA*
(Dated: October 30, 2008)

We investigate thermopower and thermoelectric coefficient of nano-granular materials at large tunneling conductance between the grains, $g_T \gg 1$. We show that at intermediate temperatures, $T \geq g_T\delta$, where δ is the mean energy level spacing for a single grain, electron-electron interaction leads to an increase of the thermopower with decreasing grain size. We discuss our results in the light of new types of thermoelectric materials and present the behavior of the figure of merit depending on system parameters.

PACS numbers: 73.63.-b, 72.15.Jf, 73.23.Hk

The search for more efficient thermoelectric materials has had little success during the last several decades since bulk materials are limited in their performance by the Wiedemann-Franz law that connects electric to thermal conductivity in such a way as to defeat all attempts at improving the dimensionless figure of merit $ZT = S^2\sigma T/\kappa$, where S is the thermopower or Seebeck coefficient, σ is the electric conductivity, and κ is the thermal conductivity [1, 2, 3, 4, 5]. To be competitive compared with conventional refrigerators, one must develop thermoelectric materials with $ZT > 2$. Although it is possible in principle to develop homogeneous materials with $ZT > 2$, there are no candidate materials on the horizon. Thus, one needs to search for *inhomogeneous/granular* thermoelectric materials in which one can directly control the system parameters.

Most theoretical progress was archived by numerical solution of phenomenological models [6, 7]. However, no analytical results obtained from a microscopic model for coupled nanodot/grain systems is available till now. Thus, the fundamental question that remains open is how thermoelectric coefficient and thermopower behave in nanogranular thermoelectric materials. Here, we make the first step towards answering this question for granular metals at intermediate temperatures by generalizing our approach [8] recently developed for the description of electric [9] and heat transport [10]. In particular, we will answer the question to what extend quantum and confinement effects in nanostructures are important in changing ZT.

In this paper we investigate the thermopower S, thermoelectric coefficient η, and the figure of merit ZT of granular samples focusing on the case of large tunneling conductance between the grains, $g_T \gg 1$. Without Coulomb interaction the granular system would be a good metal in this limit and our task is to include charging effects in the theory.

Main results.— The main results of our work are as follows: (i) We derive the expression for the thermoelectric coefficient η of granular metals that includes corrections due to Coulomb interaction at temperatures $T > g_T\delta$, where δ is the mean level spacing of a single grain

$$\eta = \eta^{(0)}\left(1 - \frac{1}{4g_Td}\ln\frac{g_TE_c}{T}\right). \qquad (1)$$

Here $\eta^{(0)} = -(\pi^2/3)eg_Ta^{2-d}(T/\varepsilon_F)$ is the thermoelectric coefficient of granular materials in the absence of electron-electron interaction with e being the electron charge, a the size of a single grain, $d = 2, 3$ the dimensionality of a sample, ε_F being the Fermi energy, and $E_c = e^2/a$ is the charging energy.

(ii) We obtain the expression for thermopower S of granular metals

$$S = S^{(0)}\left(1 - \frac{\pi-2}{4\pi g_Td}\ln\frac{g_TE_c}{T}\right), \qquad (2)$$

where $S^{(0)} = -(\pi^2/6)(1/e)(T/\varepsilon_F)$ is the thermopower of granular metals in the absence of Coulomb interaction.

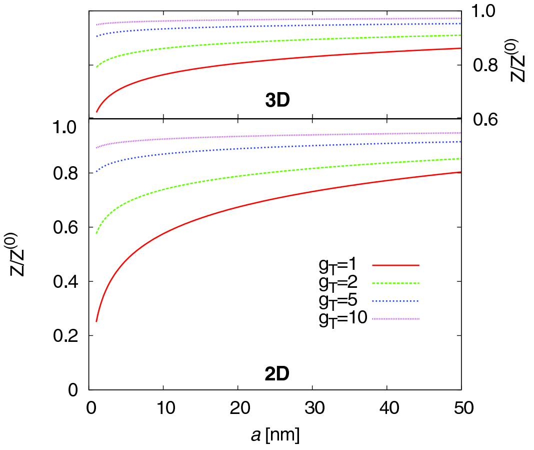

FIG. 1: Plots of the dimensionless figure of merit $Z/Z^{(0)}$ vs. grain size a (in nm)- for different values of dimensionless tunneling conductance g_T (see legend): the upper panel is for 3D and the lower for 2D. All curves are plotted for $T = 100$K. At this temperature, the dimensionless bare figure of merit for granular metals is $Z^{(0)}T \approx 10^{-4}$.

(iii) Finally, we find the figure of merit to be:

$$\frac{Z}{Z^{(0)}} = 1 - \frac{\pi - 2}{2\pi g_T d} \ln\frac{g_T E_c}{T} - \frac{1}{2\pi^2 g_T} \left\{ \begin{array}{ll} 3\gamma, & d = 3 \\ \ln\frac{g_T E_c}{T}, & d = 2 \end{array} \right. , \tag{3}$$

where $Z^{(0)}T = (\pi^2/12)(T/\varepsilon_F)^2$ is the bare figure of merit of granular materials and $\gamma \approx 0.355$ is a numerical coefficient. In Fig. 1 we plot $Z/Z^{(0)}$ as a function of the grain size a for different tunneling conductances g_T at fixed temperature 100K. We find, that the influence of granularity is most effective for small grain sizes and the presence of Coulomb interaction decreases the figure of merit.

At this point we remark that all results are obtained in the absence of phonons which become relevant only at higher temperatures. At the end of this paper we will briefly discuss their influence.

Our main results, Eqs. (1) - (3), are valid at intermediate temperatures, $T > g_T\delta$. At these temperatures the electronic motion is coherent within the grains, but coherence does not extend to scales larger than the size a of a single grain [8]. Under these conditions, the electric conductivity σ and the electric thermal conductivity κ are given by the expressions [9, 10, 11]

$$\frac{\sigma}{\sigma^{(0)}} = 1 - \ln(g_T E_c/T)/(2\pi d g_T), \tag{4a}$$

$$\frac{\kappa}{\kappa^{(0)}} = 1 - \frac{\ln[g_T E_c/T]}{2\pi d g_T} + \frac{1}{2\pi^2 g_T} \left\{ \begin{array}{ll} 3\gamma, & d = 3 \\ \ln\frac{g_T E_c}{T}, & d = 2 \end{array} \right. \tag{4b}$$

where $\sigma^{(0)} = 2e^2 g_T a^{2-d}$ and $\kappa^{(0)} = L_0 \sigma^{(0)} T$ are the electric (including spin) and thermal conductivities of granular metals in the absence of Coulomb interaction with $L_0 = \pi^2/3e^2$ being the Lorentz number. We mention that at temperature $T > g_T\delta$ the correction to the thermoelectric coefficient, Eq. (1), has a $T\ln T$ dependence in both $d = 2, 3$ dimensions which is similar to the result for the electric conductivity, Eq. (4a), having a $\ln T$ dependence in all dimensions as well.

Model.— Next we introduce our model and describe the derivation of Eqs. (1)-(3): We consider a $d-$dimensional array of metallic grains with Coulomb interaction between electrons. The motion of electrons inside the grains is diffusive and they can tunnel from grain to grain. We assume that the sample would be a good metal in the absence of Coulomb interaction. However, we also assume that g_T is still smaller than the grain conductance g_0, meaning that the granular structure is pronounced and the resistivity is controlled by tunneling between grains.

Each grain is characterized by two energy scales: (i) the mean energy level spacing δ, and (ii) the charging energy $E_c = e^2/a$ (for a typical grain size of $a \approx 10$nm E_c is of the order of 2000K) and we assume that the condition $\delta \ll E_c$ is fulfilled.

The system of coupled metallic grains is described by the Hamiltonian $\hat{H} = \sum_i \hat{H}_i$, where the sum is taken over all grains in the system and

$$\hat{H}_i = \sum_k \xi_k \hat{a}^\dagger_{i,k}\hat{a}_{i,k} + \sum_{j \neq i} \frac{e^2 \hat{n}_i \hat{n}_j}{2C_{ij}} + \sum_{j,p,q} (t^{pq}_{ij} \hat{a}^\dagger_{i,p}\hat{a}_{j,q} + \text{c.c.}). \tag{5}$$

The first term in the right hand side (r. h. s.) of Eq. (5) describes the i-th isolated disordered grain, $\hat{a}^\dagger_{i,k}(\hat{a}_{i,k})$ are the creation (annihilation) operators for an electron in the state k and $\xi_k = k^2/2m - \mu$ with μ being the chemical potential. The second term describes the charging energy, C_{ij} is the capacitance matrix and $\hat{n}_i = \sum_k \hat{a}^\dagger_{i,k}\hat{a}_{i,k}$ is the number operator for electrons in the i-th grain. The last term is the tunnel Hamiltonian where t_{ij} are the tunnel matrix elements between grains i and j.

Derivation of kinetic coefficients.— The kinetic coefficients: electric conductivity σ, the thermoelectric coefficient η, and the thermal conductivity κ are related to the Matsubara response functions $L^{(\alpha\beta)}$ with $\alpha, \beta \in \{e, h\}$ [3, 4, 12]

$$\begin{aligned} \mathbf{j}^{(e)} &= -(L^{(ee)}/(e^2T))\,\nabla(eV) - (L^{(eh)}/(eT^2))\,\nabla T, \\ \mathbf{j}^{(h)} &= -(L^{(eh)}/(eT))\,\nabla(eV) - (L^{(hh)}/T^2)\,\nabla T. \end{aligned} \tag{6}$$

Here $\mathbf{j}^{(e)}$ ($\mathbf{j}^{(h)}$) is the electric (thermal) current and V the electrostatic potential. From Eq. (6) one finds that $\sigma = L^{(ee)}/T$, $\eta = L^{(eh)}/T^2$, and $S = -\Delta V/\Delta T = L^{(eh)}/(TL^{(ee)})$, where the response functions are given by Kubo formulas $L^{(\alpha\beta)} = -\frac{\imath T\,\partial}{a^d\partial\Omega}\Big|_{\Omega\to 0} \left[\int\limits_0^{1/T} d\tau\, e^{\imath\Omega_m\tau} \langle T_\tau \mathbf{j}^{(\alpha)}(\tau)\mathbf{j}^{(\beta)}(0)\rangle \right]_{\Omega_m \to -\imath\Omega+\delta}$, with T_τ being the time ordering operator for the currents with respect to the imaginary time τ. Thus, to calculate the thermoelectric coefficient η and thermopower S of the granular metals one has to know the explicit form of the electric $\mathbf{j}^{(e)}$ and thermal $\mathbf{j}^{(h)}$ currents.

The electric current $\mathbf{j}^{(e)}_i$ through grain i is defined as $\mathbf{j}^{(e)}_i = \sum_j \hat{\jmath}^{(e)}_{ij} = e\, d\hat{n}_i/dt = \imath e[\hat{n}_i, \hat{H}]$. Straightforward calculations lead to $\hat{\jmath}^{(e)}_{ij} = \imath e \sum_{k,q} (t^{kq}_{ij} \hat{a}^\dagger_{i,k}\hat{a}_{j,q} - t^{qk}_{ji} \hat{a}^\dagger_{j,q}\hat{a}_{i,k})$.

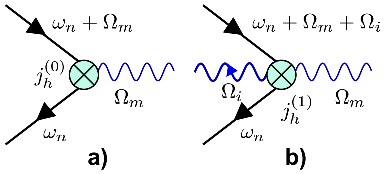

FIG. 2: Vertices corresponding to the thermal current operator, Eqs. (7): vertex (a) corresponds to $\widehat{\jmath}^{(h,0)}_{ij}$ and (b) to $\widehat{\jmath}^{(h,1)}_{ij}$. The solid lines denote the propagator of electrons, the thick wavy line describes Coulomb interaction, the tunneling vertices are described by the circles, $\omega_n = \pi T(2n+1)$ and $\Omega_m = 2\pi m T$ are Fermionic and Bosonic Matsubara frequencies respectively ($n, m \in \mathbb{Z}$).

For granular metals the thermal current operator $\mathbf{j}_i^{(h)} = \sum_j \hat{\jmath}_{ij}^{(h)}$ can be obtained as follows. The energy content of each grain changes as a function of time, such that $d\hat{H}_i/dt = i[\hat{H}_i, \hat{H}]$. Energy conservation requires that this energy flow to the other grains in the system, $d\hat{H}_i/dt \equiv \sum_j \hat{\jmath}_{ij}^{(h)}$. Calculating the commutator $[\hat{H}_i, \hat{H}]$, we obtain $\hat{\jmath}_{ij}^{(h)} = \hat{\jmath}_{ij}^{(h,0)} + \hat{\jmath}_{ij}^{(h,1)}$, where

$$\hat{\jmath}_{ij}^{(h,0)} = \imath \sum_{k,q} \frac{\xi_k + \xi_q}{2} \left[t_{ij}^{kq} \hat{a}^\dagger_{i,k} \hat{a}_{j,q} - t_{ji}^{qk} \hat{a}^\dagger_{j,q} \hat{a}_{i,k} \right], \tag{7a}$$

$$\hat{\jmath}_{ij}^{(h,1)} = -\frac{e}{4} \sum_m \left[\frac{\{\hat{n}_i; \hat{\jmath}_{jm}^{(e)}\}_+}{C_{im}} - \frac{\{\hat{n}_j; \hat{\jmath}_{im}^{(e)}\}_+}{C_{jm}} \right], \tag{7b}$$

where $\{\hat{A}; \hat{B}\}_+$ stands for the anti-commutator. The contribution $\hat{\jmath}_{ij}^{(h,0)}$ is the heat current in the absence of electron-electron interaction, while the second term $\hat{\jmath}_{ij}^{(h,1)}$ appears due to Coulomb interaction. Equations (7) imply that the thermal current operator must be associated with two different vertices in diagram representation, Fig. 2.

For large tunneling conductance, the Matsubara thermal current - electric current correlator can be analyzed perturbatively in $1/g_T$, using the diagrammatic technique discussed in Ref. 8 that we briefly outline below. The self-energy of the averaged single electron Green function has two contributions: The first contribution corresponds to scattering by impurities inside a single grain while the second is due to processes of scattering between the grains. The former results only in small renormalization of the mean free time which depends in general on the electron energy ω as $\tau_\omega^{-1} = \tau_0^{-1}[1 + (d/2 - 1)\omega/\varepsilon_F]$ which is a result of the renormalization of the density of states at the Fermi surface.

The diffusion motion inside a single grain is given by the diffusion propagator $\mathcal{D}_0^{-1} = \tau_\omega |\Omega_i|$, where Ω_i is the bosonic Matsubara frequency for the (internal) Coulomb interaction. The coordinate dependence in $\mathcal{D}_0$ is neglected since in the regime under consideration all characteristic energies are smaller than the Thouless energy. The complete diffusion propagator is given by ladder diagrams resulting in the following expression $\mathcal{D}^{-1}(\Omega_i, \mathbf{q}) = \tau_\omega(|\Omega_i| + \epsilon_{\mathbf{q}}\delta)$, where $\epsilon_{\mathbf{q}} = 2g_T \sum_{\mathbf{a}}(1 - \cos \mathbf{qa})$ with $\mathbf{a}$ being the lattice vectors. The same ladder diagrams describe the renormalized interaction vertex. The interaction vertex is used to obtain the polarization operator, that defines the effective dynamically screened Coulomb interaction for granular metals, $V(\Omega_i, \mathbf{q}) = 2\left[E_c^{-1}(\mathbf{q}) + 4\epsilon_{\mathbf{q}}/(|\Omega_i| + \epsilon_{\mathbf{q}}\delta)\right]^{-1}$, where the charging energy in $d = 2, 3$ is given by $E_c(\mathbf{q}) = \frac{e^2}{2C(\mathbf{q})} = \frac{2^d \pi e^2 q}{4(aq)^d}$.

However, there is an important difference between calculations of thermoelectric coefficient η and thermopower S and the calculations of the electric σ and thermal κ conductivities in Eqs. (4a, 4b). Indeed, to calculate σ and κ it was sufficient to approximate the tunneling matrix element t_{pq} as a constant t which is evaluated at the Fermi surface and neglect variations of t_{pq} with energy which occur on the scale T/ε_F. However, this approximation is insufficient for calculations of thermoelectric coefficient η and thermopower S since the dominant contribution to these quantities vanishes due to particle-hole symmetry such that that both quantities are proportional to the small parameter T/ε_F. Since it is necessary to take into account terms of order of T/ε_F in order to obtain a nonzero result for η and S the corresponding expansions must be carried out to this order for all quantities which depend on energy: the density of states, the relaxation time, and the tunneling matrix element. For the latter we obtain the expression: $t^2(\xi_1, \xi_2) = t_0^2\left(1 + \frac{\xi_1 + \xi_2}{\varepsilon_F}\right)$ [19].

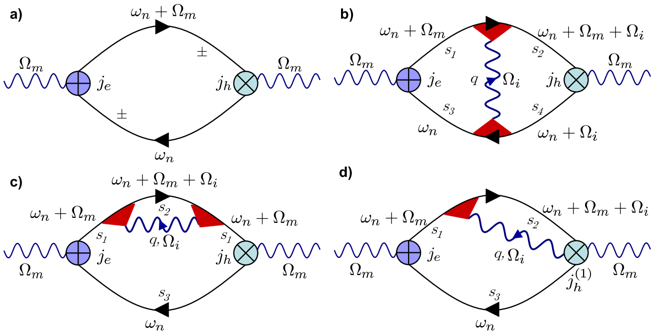

FIG. 3: Diagrams describing the thermoelectric coefficient of granular metals at temperatures $T > g_T\delta$: diagram (a) corresponds to η_0 in Eq. (1). Diagrams (b)-(d) describe first order corrections to the thermoelectric coefficient of granular metals due to electron-electron interaction. The solid lines denote the propagator of electrons, the wavy lines describe effective screened electron-electron propagator, and the (red) triangles describe the elastic interaction of electrons with impurities. The tunneling vertices are described by the circles. The sum of the diagrams (b)-(d) results in the thermoelectric coefficient correction $\eta^{(1)}$ given in Eq. (8).

In the absence of the electron-electron interaction the thermoelectric coefficient is represented by diagram (a) in Fig. 1. Straightforward calculations of this diagram lead to the result for $\eta^{(0)}$ given below Eq. (1).

First order interaction corrections to the thermoelectric coefficient are only generated by diagrams (b) and (c) in Fig. 3, resulting after summation over Fermionic and Bosonic frequencies and analytical continuation in

$$\eta^{(1)} = -\frac{\eta^{(0)}}{2\pi g_T}\left(\frac{a}{2\pi}\right)^d \int d^d\mathbf{q} \ln\left[\frac{2E_c(\mathbf{q})\epsilon_{\mathbf{q}}}{T}\right], \tag{8}$$

where the $\mathbf{q}$-integration goes over the d-dimensional sphere with radius π/a. Diagram (d) in Fig. 3 gives only contributions to the thermoelectric coefficient of order $(T/\varepsilon_F)^2$ and higher. Integrating over $\mathbf{q}$ in Eq. (8) we obtain the following expressions:

$$\eta_{2d}^{(1)} = -\frac{\eta^{(0)}}{8g_T}\ln\frac{E_c g_T}{T}, \qquad \eta_{3d}^{(1)} = -\frac{\eta^{(0)}}{12g_T}\ln\frac{E_c g_T}{T}, \tag{9}$$

which lead to Eq. (1).

Discussions.— In the presence of interaction effects and not very low temperatures $T > g_T\delta$, granular metals behave differently from homogeneous disorder metals. However, in the absence of interactions the result for $\eta^{(0)}$ below Eq. (1) coincides with the thermoelectric coefficient of homogeneous disordered metals, $\eta_{hom}^{(0)} = -(2/9)ep_F(\tau_0 T)$, with p_F being the Fermi momentum. One can expect that at low temperatures, $T < g_T\delta$, even in the presence of Coulomb interaction the behavior of thermoelectric coefficient and thermopower of granular metals is similar to the behavior of η_{hom} and S_{hom}, however this temperature range is beyond the scope of the present paper . Our results for thermopower (2) and figure of merit (3) show that the influence of Coulomb interaction is most effective for small grains. S^2 decreases with the grain size which is a result of the delicate competition of the corrections of thermoelectric coefficient (1) and the electric conductivity (4a). In particular, if the numerical prefactor of the correction to η would be slightly smaller, the sign of the correction to S would change.

Above we only considered the electron contribution to figure of merit. At higher temperatures $T > T^*$, where $T^* \sim \sqrt{g_T c_{ph}^2/l_{ph}a}$ is a characteristic temperature with l_{ph} and c_{ph} being the phonon scattering length and phonon velocity respectively [10], phonons will provide an independent, additional contribution to thermal transport, $\kappa_{ph} = T^3 l_{ph}/c_{ph}^2$. However, the phonon contribution can be neglected for temperatures $g_T\delta < T < T^*$. A detailed study of the influence of phonons at high temperatures, including room temperature, will be subject of a forthcoming work.

So far, we ignored the fact that electron-electron interactions also renormalize the chemical potential μ. In general, this renormalization may affect the kinetic coefficients: the thermal current vertex, Fig 2, as well as the electron Green functions depend on μ. In particular one needs to replace $\nabla(eV) \to \nabla(eV + \mu)$ in Eqs. (6). To first order in the interactions, the renormalization of μ only leads to corrections to diagram (a) in Fig. 3. As it can be easily shown, for this diagram the renormalization of the heat and electric current vertices is exactly canceled by the renormalization of the two electron propagators. Therefore, the renormalization of the chemical potential does not affect our results in the leading order.

Finally, we remark that the bare figure of merit $Z^{(0)}T$ for granular metals at $g_T > 1$ and 100K is of the order of only 10^{-4}. Therefore these materials are not suitable for *solid-state refrigerators*, but should be replaced by granular semiconductors with $g_T < 1$. Therefore we conclude this paragraph discussing the dimensionless figure of merit ZT of granular materials at weak coupling between the grains, $g_T \ll 1$. In this regime the electronic contribution to thermal conductivity κ_e of granular metals was recently investigated in Ref. 13, where it was shown that $\kappa_e \sim g_T^2 T^3/E_c^2$. In this regime the electric conductivity of granular metals obeys the law $\sigma \sim g_T \exp(-E_c/T)$ [8, 11]. However, an expression for the thermoelectric coefficient in this region is not available yet, but recently it has been proposed, based on experiment, that nanostructured thermoelectric materials in the low coupling region ($\mathrm{AgPb}_m\mathrm{SbTe}_{2+m}$, $\mathrm{Bi_2Te_3/Sb_2Te_3}$, or $\mathrm{CoSb_3}$) [14, 15, 16, 17, 18] can have higher figures of merit than their bulk counterparts.

In conclusion, we have investigated the thermoelectric coefficient and thermopower of granular nanomaterials in the limit of large tunneling conductance between the grains and temperatures $T > g_T\delta$. We have shown to what extend quantum and confinement effects in granular metals are important in changing ZT depending on system parameters.

Acknowledgements.— We thank Frank Hekking, Nick Kioussis, and Gang Lu for useful discussions. A. G. was supported by the U.S. Department of Energy Office of Science under the Contract No. DE-AC02-06CH11357.

[1] D. M. Rowe and C. M. Bhandari, Modern thermoelectrics (Reston, Reston, VA, 1983).

[2] A. A. Abrikosov, Fundamentals of the theory of metals (North Holland, Amsterdam, 1988).

[3] G. D. Mahan, Many-particle phyics, (Kluwer, New York, 2000)

[4] G. D. Mahan, J. Appl. Phys. **70**, 4551 (1991).

[5] L. E. Bell, Science **321**, 1457 (2008).

[6] T. E. Humphrey and H. Linke, Phys. Rev. Lett. **94**, 096601 (2005).

[7] D. A. Broido and T. L. Reinecke, Phys. Rev. B **51**, 13797 (1995).

[8] I. S. Beloborodov, *et al,* Rev. Mod. Phys. **79**, 469 (2007).

[9] I. S. Beloborodov, *et al,* Phys. Rev. Lett. **91**, 246801 (2003).

[10] I. S. Beloborodov, *et al,* Europhys. Lett. **69**, 435 (2005).

[11] K. B. Efetov and A. Tschersich, Europhys. Lett. **59**, 114, (2002); Phys. Rev. B **67**, 174205 (2003).

[12] M. Jonson and G. D. Mahan, Phys. Rev. B **21**, 4223 (1980).

[13] V. Tripathi and Y. L. Loh, Phys. Rev. Lett. **96**, 046805 (2006).

[14] K. F. Hsu *et al,* Science **303**, 816 (2004).

[15] A. Majumdar, Science **303**, 777 (2004).

[16] B. Poudel *et al,* Science **320**, 634 (2008).

[17] J. L. Min *et al,* Appl. Phys. Lett. **91**, 172116 (2007).

[18] T. C. Harman *et al,* Science **297**, 2229 (2002).

[19] The energy dependent expression for the tunneling matrix element includes the effect of multi-channel tunneling.